

Multi-dimensional Preference Alignment by Conditioning Reward Itself

Jiho Jang¹ Jinyoung Kim Kyungjune Baek^{2,†} Nojun Kwak^{1,†}
¹Seoul National University ²Sejong University
 {geographic, nojunk}@snu.ac.kr kyungjune.baek@sejong.ac.kr

Abstract

Reinforcement Learning from Human Feedback has emerged as a standard for aligning diffusion models. However, we identify a fundamental limitation in the standard DPO formulation because it relies on the Bradley-Terry model to aggregate diverse evaluation axes like aesthetic quality and semantic alignment into a single scalar reward. This aggregation creates a reward conflict where the model is forced to unlearn desirable features of a specific dimension if they appear in a globally non-preferred sample. To address this issue, we propose Multi Reward Conditional DPO (MCDPO). This method resolves reward conflicts by introducing a disentangled Bradley-Terry objective. MCDPO explicitly injects a preference outcome vector as a condition during training, which allows the model to learn the correct optimization direction for each reward axis independently within a single network. We further introduce dimensional reward dropout to ensure balanced optimization across dimensions. Extensive experiments on Stable Diffusion 1.5 and SDXL demonstrate that MCDPO achieves superior performance on benchmarks. Notably, our conditional framework enables dynamic and multiple-axis control at inference time using Classifier Free Guidance to amplify specific reward dimensions without additional training or external reward models.

1. Introduction

Reinforcement Learning from Human Feedback (RLHF) [15], a technique that aligns model outputs with human preferences, has emerged as a key component in large-scale language model (LLM) training pipelines [12, 14, 28]. Recent research extends RLHF to generative image models [1, 9, 27]. In particular, Diffusion-DPO [23] is a method that applies Direct Preference Optimization (DPO) [18] to diffusion models. It is widely adopted for its ability to align models using only binary win-lose labels via the Bradley-Terry (BT) model.

[†]Co-corresponding authors.

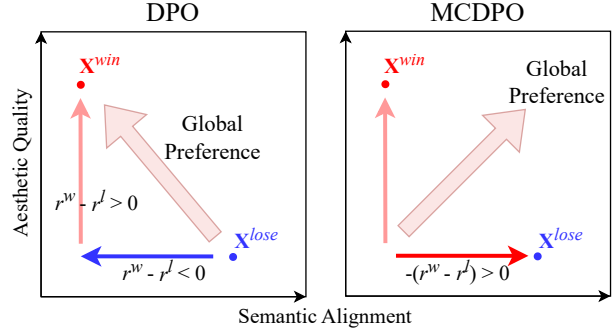


Figure 1. DPO suffers from reward conflicts ($r^w - r^l < 0$) when global preference contradicts a specific dimension. MCDPO resolves this by disentangling axes to learn the correct direction for each dimension independently ($-(r^w - r^l) > 0$).

However, while a single image sample can possess various evaluation axes such as aesthetic quality, prompt fidelity, and safety, the BT model relies solely on a single win-lose label for the entire sample. This formulation makes it difficult to control or reflect specific, multi-dimensional preference axes during training. This fundamental conflict arises from the standard BT model’s formulation, which models global preference as a linear combination of multiple reward axes. Consequently, when presented with a sample pair that is a global win but a local lose on a specific dimension j , the model is forced to learn in the opposite direction of the intended preference for that dimension. Existing studies in the LLM field address this by: (1) dynamically combining model parameters based on reward weights [24], (2) regularizing to gradients that align with the prior preference [13], or (3) in-context reward modeling via SFT [29]. In the diffusion domain, a common strategy is to consider only the samples that are dominant across all axes as preferred [4, 10]. Nevertheless, these approaches fail to resolve the fundamental conflict within the DPO loss formulation. Consequently, they provide a limited learning signal and are sample-inefficient.

To resolve the issue, we first propose a disentangled BT objective, which models preferences independently for each dimension by explicitly introducing a preference outcome vector that indicates the actual win, lose, or tie status for each axis. This formulation ensures every dimen-

sion is optimized in the correct direction, resolving the ambiguity in conflicting pairs. Our practical implementation, Multi-reward Conditional Direct Preference Optimization (MCDPO), injects this preference outcome vector itself as a condition during the DPO loss calculation. This conditional approach transforms the problematic reward-conflict pairs into a powerful supervision signal for disentanglement, allowing the model to learn to optimize for each reward axis independently within a single network (See Figure 1).

By resolving the reward conflict, we experimentally demonstrate that MCDPO outperforms baselines and forms robust, efficient feature representations for each alignment axis. Furthermore, the proposed conditional model provides a significant advantage at inference time. By leveraging the preference condition, the trained model can utilize Classifier-Free Guidance (CFG) [5] to measure and amplify the score function towards higher-reward outcomes, enabling dynamic, multi-axis control during generation.

In summary, the main contributions are as follows:

- We propose the disentangled BT objective and its practical implementation, Multi-reward Conditional DPO (MCDPO), to address the known reward conflict problem in BT-based DPO. Our method uses a preference outcome vector as a condition to disentangle reward axes.
- We experimentally show that MCDPO achieves superior performance and sample efficiency, learning robust representations for each alignment axis.
- We showcase MCDPO’s conditional structure, which enables dynamic, multi-axis control during inference using Classifier-Free Guidance.

2. Background

2.1. Diffusion Models

Diffusion models are a class of generative models that learn to generate data by reversing a gradual noising process. [6] The forward process progressively adds Gaussian noise to data \mathbf{x}_0 over T timesteps:

$$q(\mathbf{x}_t|\mathbf{x}_{t-1}) = \mathcal{N}(\mathbf{x}_t; \sqrt{1 - \beta_t}\mathbf{x}_{t-1}, \beta_t\mathbf{I}), \quad (1)$$

where β_t is a variance schedule. The reverse process learns to denoise by training a neural network ϵ_θ to predict the noise at each timestep. The training objective is:

$$\mathcal{L} = \mathbb{E}_{t, \mathbf{x}_0, \epsilon} [\|\epsilon - \epsilon_\theta(\mathbf{x}_t, t, c)\|^2], \quad (2)$$

where c represents conditioning information (e.g., text prompt), and $\epsilon \sim \mathcal{N}(0, \mathbf{I})$ is the added noise to \mathbf{x}_0 .

At inference, sampling starts from pure noise $\mathbf{x}_T \sim \mathcal{N}(0, \mathbf{I})$ and iteratively denoises to generate \mathbf{x}_0 . The learned score function $\nabla_{\mathbf{x}} \log p_\theta(\mathbf{x}_t|c)$ guides this reverse process. [21] Classifier-Free Guidance (CFG) [5] strengthens conditioning by modifying the score function:

$$\nabla_{\mathbf{x}} \log p_\theta(\mathbf{x}_t) + \lambda_{\text{cfg}} (\nabla_{\mathbf{x}} \log p_\theta(\mathbf{x}_t|c) - \nabla_{\mathbf{x}} \log p_\theta(\mathbf{x}_t)), \quad (3)$$

where λ_{cfg} controls guidance strength. By amplifying the score difference, CFG enhances adherence to the conditioning signal c .

2.2. DPO in Diffusion Models

Direct Preference Optimization (DPO) [18] offers a simplified approach to aligning generative models with human preferences by directly optimizing policy models without requiring explicit reward models. DPO leverages the Bradley-Terry (BT) model [2] to model preference probabilities from pairwise comparisons. Given a pair of samples \mathbf{x}^w (preferred) and \mathbf{x}^l (less preferred) conditioned on prompt c , the BT model defines:

$$p_{\text{BT}}(\mathbf{x}^w > \mathbf{x}^l|c) = \sigma(r(\mathbf{x}^w, c) - r(\mathbf{x}^l, c)), \quad (4)$$

where $\sigma(\cdot)$ is the sigmoid function and $r(\mathbf{x}, c)$ is a reward function.

A key insight of DPO is that the reward can be expressed analytically in terms of the learned policy p_θ and a reference policy p_{ref} :

$$r(\mathbf{x}, c) = \beta \log \left(\frac{p_\theta(\mathbf{x}|c)}{p_{\text{ref}}(\mathbf{x}|c)} \right) + \beta \log Z(c), \quad (5)$$

where β is a KL regularization parameter and $Z(c)$ is the partition function. This formulation allows DPO to optimize preferences directly through the policy without training a separate reward model.

For diffusion models [23], the DPO objective operates at the denoising transition level. Given a preference (win-lose) pair $(\mathbf{x}^w, \mathbf{x}^l)$, the loss function is:

$$\begin{aligned} \mathcal{L}_{\text{DPO}} &= -\mathbb{E} \log \sigma \left(\beta \log \frac{p_\theta(\mathbf{x}_t^w|\mathbf{x}_{t+1}^w, c)}{p_{\text{ref}}(\mathbf{x}_t^w|\mathbf{x}_{t+1}^w, c)} - \beta \log \frac{p_\theta(\mathbf{x}_t^l|\mathbf{x}_{t+1}^l, c)}{p_{\text{ref}}(\mathbf{x}_t^l|\mathbf{x}_{t+1}^l, c)} \right) \\ &= -\mathbb{E} \log \sigma(-\beta T \omega_t (\|\epsilon^w - \epsilon_\theta(\mathbf{x}_t^w, t)\| - \|\epsilon^w - \epsilon_{\text{ref}}(\mathbf{x}_t^w, t)\| \\ &\quad - (\|\epsilon^l - \epsilon_\theta(\mathbf{x}_t^l, t)\| - \|\epsilon^l - \epsilon_{\text{ref}}(\mathbf{x}_t^l, t)\|)), \end{aligned} \quad (6)$$

where the expectation is over timesteps t and noisy samples from the diffusion forward process. This formulation trains the diffusion model to increase the likelihood of preferred samples while decreasing that of less preferred ones, relative to the reference policy.

In practice, generated samples are evaluated along multiple distinct axes, such as aesthetic quality, semantic alignment, and safety. However, the standard BT model aggregates these into a single scalar reward by a linear combination of different dimensions:

$$r(\mathbf{x}, c) = \sum_{i=1}^D w_i r_i(\mathbf{x}, c), \quad (7)$$

where r_i represents the reward for dimension i and w_i its weight. This leads to a fundamental reward conflict: when x^w is preferred globally but performs worse than x^l on a

specific dimension j , the DPO loss may inadvertently degrade that dimension as shown in Figure 1 (Left).

Existing studies attempt to address or bypass this issue. In the LLM field, prominent approaches include: (1) dynamically combining expert model parameters based on user-specified reward weights [24], (2) train the model sequentially by applying regularization to align gradients with prior preferences [13], or (3) circumventing the DPO conflict entirely by using Supervised Fine-Tuning (SFT) leverages reward scores within the prompt [29]. In the diffusion domain, a common strategy to avoid this conflict is to generate images until the samples that are dominant across all axes as preferred [4, 10]. Nevertheless, these approaches fail to resolve the fundamental conflict within the DPO loss formulation itself. By either training only on non-conflicting pairs (which is sample-inefficient) or using alternative objectives (like SFT or regularization), they rely on a limited learning signal rather than directly solving the ambiguity in DPO. In this work, we aim to analyze the problem and resolve the limitations.

3. Method

In this section, we describe a framework to address the reward conflict inherent in multi-dimensional DPO. We begin by theoretically analyzing this conflict and then introduce a disentangled Bradley-Terry objective that fundamentally resolves it in Section 3.1. Following this analysis, we introduce Multi-reward Conditional DPO (MCDPO) in Section 3.2 that leverages reward conditioning to approximate this theoretical objective using a single network. To ensure balanced optimization, in Section 3.3, we identify the potential issue of gradient domination and propose reward dropout as a robust solution. Finally, in Section 3.4, we demonstrate how our conditional framework uniquely enables dynamic, multi-axis test-time reward optimization.

3.1. Multi-reward Disentanglement

As discussed in Section 2, the standard BT model simplifies all preferences into a single, monolithic reward. This global reward is effectively a linear combination of the individual reward axes as follows:

$$p_{BT}(\mathbf{x}^w > \mathbf{x}^l | c) = \sigma \left[\sum_i w_i (r_i(\mathbf{x}^w, c) - r_i(\mathbf{x}^l, c)) \right]. \quad (8)$$

This formulation leads to a fundamental reward conflict where a sample x^w is preferred globally but performs worse than x^l on a specific dimension j (i.e., $r_j(x^w) < r_j(x^l)$). Because the standard DPO loss optimizes for the global win, it is forced to learn in the opposite direction of the intended preference for dimension j , actively degrading that specific quality. To resolve this, we first introduce a disentangled Bradley-Terry objective. The core idea is to model the preference for each dimension independently. We explicitly introduce a preference outcome vector $\gamma \in \mathbb{R}^D$,

where each element γ_i indicates the estimated reward of win(+1), lose(-1), or tie(0) for each axis i :

$$\gamma_i(x, y) = \begin{cases} 1 & \text{if } r_i(x) > r_i(y) \\ 0 & \text{if } r_i(x) = r_i(y) \\ -1 & \text{if } r_i(x) < r_i(y). \end{cases} \quad (9)$$

The vector, γ , is then used to modify the objective as follows:

$$\begin{aligned} p_{BT}^\perp(\mathbf{x}^w > \mathbf{x}^l | c, \gamma(\mathbf{x}^w, \mathbf{x}^l)) \\ = \sigma \left[\sum_i w_i \gamma_i(\mathbf{x}^w, \mathbf{x}^l) (r_i(\mathbf{x}^w, c) - r_i(\mathbf{x}^l, c)) \right] \geq p_{BT}(\mathbf{x}^w > \mathbf{x}^l | c), \end{aligned} \quad (10)$$

where equality only holds when all dimensions agree.

This formulation ensures each dimension is optimized in the correct direction. If the j -th dimensional preference is inverted (e.g., x^l wins on aesthetics), γ_j becomes negative, which flips the sign for that dimension’s gradient. By doing so, we can fundamentally resolve the ambiguity in conflicting pairs and ensure all dimensions provide correct supervision to the model [3, 22, 25].

3.2. Multi-reward Conditional DPO

While training a model D times sequentially for each reward axis is a straightforward way to implement the disentangled objective:

$$r_i(\mathbf{x}, c) = \beta \log \left(\frac{p_i(\mathbf{x}|c)}{p_{\text{ref}}(\mathbf{x}|c)} \right) + \beta \log Z(c) \quad (11)$$

this approach would require optimizing a loss:

$$L_M = -\mathbb{E} \log \sigma \left[\beta \sum_i w_i \gamma_i \left(\log \frac{p_i(\mathbf{x}^w|c)}{p_{\text{ref}}(\mathbf{x}^w|c)} - \log \frac{p_i(\mathbf{x}^l|c)}{p_{\text{ref}}(\mathbf{x}^l|c)} \right) \right], \quad (12)$$

which has two major drawbacks. First, it requires training D separate models (or D forward passes if using dimension indicators $\hat{\gamma}_i$ as $p_i = p(\cdot | \hat{\gamma}_i)$), which is computationally prohibitive. Second, it does not fundamentally resolve conflicts, as each model is still trained on pairs where its dimension may conflict with others.

To resolve this, we propose Multi-reward Conditional DPO (MCDPO), an efficient solution that models p_{BT}^\perp (Equation (10)) using a single conditional diffusion model. The key insight is to reframe the objective from an explicit sign-flip (Equation (12)) to a learned function approximation task. We leverage the core DPO principle that the policy is an implicit reward model, but define a conditional implicit reward: $r_\theta(\mathbf{x}, c, \gamma) = \beta \log(p(\mathbf{x}|c, \gamma)/p_{\text{ref}}(\mathbf{x}|c))$. Our final loss, L_{MC} (Equation (13)), trains this single $r_\theta(\mathbf{x}, c, \gamma)$ to emulate the behavior of the entire theoretical, disentangled ensemble from Equation (12).

By conditioning on γ , we convert reward-conflict pairs from a problem into a powerful learning signal. For example, when the model is given a pair and the condition $\gamma = [\text{aesthetic: win, semantic: lose}]$, it should learn to recognize

that x^w is aesthetically superior while x^l has better semantic alignment. It is only possible if the model learns to represent these preference axes independently. When trained on sufficient conflict pairs, the model learns to disentangle each reward dimension, effectively training D implicit reward models within a single model. To maximize data efficiency, our final loss function, L_{MC} , exploits the symmetry of preferences by training on both pair orientations as follows:

$$L_{MC} = -\mathbb{E} \log \sigma \left[\left(\beta \log \frac{p(\mathbf{x}^w|c, \gamma^{wl})}{p_{\text{ref}}(\mathbf{x}^w|c)} - \beta \log \frac{p(\mathbf{x}^l|c, \gamma^{wl})}{p_{\text{ref}}(\mathbf{x}^l|c)} \right) + \left(\beta \log \frac{p(\mathbf{x}^l|c, \gamma^{lw})}{p_{\text{ref}}(\mathbf{x}^l|c)} - \beta \log \frac{p(\mathbf{x}^w|c, \gamma^{lw})}{p_{\text{ref}}(\mathbf{x}^w|c)} \right) \right] \quad (13)$$

where γ^{wl} and γ^{lw} denote $\gamma(x^w, x^l)$ and $\gamma(x^l, x^w)$, respectively. To feed γ into the model, we devise a reward conditioning module described in Section 3.5.

3.3. Mitigating Gradient Domination

While our L_{MC} objective Equation (13) successfully disentangles reward axes, naively training with it can lead to gradient domination. This occurs when dimensions that are easier to learn suppress the learning signals for harder dimensions, leading to unbalanced optimization.

Analyzing the exact gradient of L_{MC} (Equation (13)) is complex. Since L_{MC} aims to approximate the theoretical objective L_M (Equation (12)), we can conceptually understand this phenomenon by analyzing the gradient of L_M instead.

Formally, by replacing $p_i(\cdot) = p_\theta(\cdot|\hat{\gamma}_i)$, we can write the gradient of the loss as follows:

$$\nabla_{\theta} L = (\sigma(z) - 1) \nabla_{\theta} z, \quad \nabla_{\theta} z = \sum_i \beta w_i (\nabla_{\theta} \log p_\theta(\mathbf{x}^w|c, \hat{\gamma}_i) - \nabla_{\theta} \log p_\theta(\mathbf{x}^l|c, \hat{\gamma}_i)) \quad (14)$$

where z aggregates the per-dimension log-likelihood ratios. We can find two sources of the issue. First, if any single dimension becomes highly confident, $\sigma(z) \rightarrow 1$, the global gradient goes to zero; therefore, the entire training converges to the local optima. Second, within $\nabla_{\theta} z$, if the model becomes highly discriminative for dimension i , which causes a large gradient norm for that dimension; it can dominate the sum and overwhelm gradients from other dimensions.

To address this, we introduce dimensional reward dropout. During training, we randomly drop individual reward dimensions by setting their condition $\gamma_i = 0$. By doing so, we can zero out the contribution of the dropped dimension to both the $\sigma(z)$ term and the summed gradient $\nabla_{\theta} z$. This simple technique prevents any single dimension from consistently dominating the training signal, ensuring balanced optimization across all axes.

3.4. Test-time Reward Optimization

A significant advantage of our conditional framework is that it enables dynamic, multi-axis reward optimization at inference time. Our training objective implicitly guides the model to represent two distinct distributions, including the distribution of preferred samples $p(\mathbf{x}|c, \gamma^w)$ and the distribution of non-preferred samples $p(\mathbf{x}|c, \gamma^l)$.

$$p(\mathbf{x}|c, \gamma^w) = p_{\text{ref}}(\mathbf{x}|c) \exp(r^w(\mathbf{x}, c)/\beta) / Z(c) \quad (15)$$

This structure is a natural fit for Classifier-Free Guidance (CFG). By computing the difference between the score functions for the ‘‘win’’ and ‘‘lose’’ conditions, we can derive the gradient of the implicit reward difference ($r^w - r^l$):

$$\nabla_{\mathbf{x}} \log p(\mathbf{x}|c, \gamma^w) - \nabla_{\mathbf{x}} \log p(\mathbf{x}|c, \gamma^l) = \nabla_{\mathbf{x}} (r^w - r^l) / \beta \quad (16)$$

The gradient can then be incorporated into the standard CFG sampling process as follows:

$$\nabla_{\mathbf{x}} \log p(\mathbf{x}|\gamma^l) + \lambda_{\text{cfg}} (\nabla_{\mathbf{x}} \log p(\mathbf{x}|c, \gamma^w) - \nabla_{\mathbf{x}} \log p(\mathbf{x}|\gamma^l)) \quad (17)$$

By doing so, we can steer the generation process away from the non-preferred (γ^l) and toward the preferred (γ^w). This enables fine-grained, dynamic control, allowing a user to specify a weighted combination of preference gradients at test time without requiring any external reward models.

3.5. Context-aware Reward Conditioning

We encode the preference outcome vector γ as natural language tokens (e.g., ‘‘win tie’’, meaning win for aesthetic score and tie for semantic alignment) via the text encoder to get an initial embedding e_γ . This embedding is then injected into the model.

First, the U-Net latent z_t is updated using parallel cross-attention (CA) blocks with the text prompt c_{prompt} and the final context-aware reward embedding c_{reward} :

$$z'_t = \text{CA}(z_t, c_{\text{prompt}}) + \lambda \cdot \text{CA}'(z_t, c_{\text{reward}}) \quad (18)$$

where z'_t is the updated latent, CA' is a copy of the pre-trained CA module [30], and λ is a weighting scalar, which we set to 1 in all our experiments.

For dimensions requiring both text and image context (e.g., semantic alignment), the embedding c_{reward} is computed using a context-aware conditioning module. This module refines the initial γ embedding e_γ by attending to both the text prompt and the image latent sequentially:

$$h_{\text{SA}} = \text{SA}(e_\gamma, c_{\text{prompt}}), \quad h_{\text{CA}} = \text{CA}''(h_{\text{SA}}, z_t) \quad (19) \\ c_{\text{reward}} = \text{MLP}(h_{\text{CA}})$$

where SA, CA'' , and MLP are zero-initialized to preserve pretrained knowledge. This final c_{reward} embedding is then fed into Equation (18) as the input to CA' .

Table 1. Main Results on SD1.5 (win rates vs. SD1.5 baseline). * indicates the model checkpoint released by the authors. **Bold** and underline indicate the best and second-best results, respectively. We will use the same notation throughout the paper.

| Datasets | Models | PickScore | Aesthetic | HPSv2 | CLIP | ImageReward | MPS | Average |
|--------------|------------|--------------|--------------|--------------|--------------|--------------|--------------|--------------|
| PickV2 | Diff. DPO* | 75.52 | 65.08 | 70.28 | <u>57.80</u> | 64.44 | 67.33 | 66.74 |
| | Diff. KTO* | 73.40 | 71.24 | 82.24 | 56.64 | 76.04 | 69.30 | 71.48 |
| | DSPO | 76.36 | 75.88 | 81.92 | 59.16 | 77.36 | 68.80 | 73.24 |
| | MCSFT | <u>78.24</u> | <u>78.16</u> | <u>89.60</u> | 57.36 | <u>79.20</u> | <u>69.53</u> | <u>75.35</u> |
| | MCDPO | 86.20 | 91.88 | 93.44 | 57.64 | 82.92 | 76.75 | 81.47 |
| PartiPrompts | Diff. DPO* | 66.72 | 60.72 | 64.58 | 53.49 | 62.62 | 64.69 | 62.14 |
| | Diff. KTO* | 65.74 | 69.85 | <u>80.14</u> | <u>55.82</u> | 72.48 | 63.86 | 67.98 |
| | DSPO | <u>68.07</u> | 75.18 | 79.47 | 56.67 | 72.85 | 65.56 | 69.63 |
| | MCSFT | 60.42 | 68.75 | 69.18 | 48.49 | 65.63 | 60.88 | 62.22 |
| | MCDPO | 80.94 | 92.52 | 86.46 | 50.65 | 76.35 | 72.52 | 76.57 |
| HPDv2 | Diff. DPO* | 76.80 | 66.60 | 70.90 | 56.70 | 62.50 | 66.66 | 66.69 |
| | Diff. KTO* | 75.55 | 74.40 | 86.35 | 53.20 | 78.20 | 69.17 | 72.81 |
| | DSPO | <u>78.10</u> | 78.40 | <u>86.55</u> | <u>55.45</u> | <u>79.80</u> | <u>70.25</u> | 74.75 |
| | MCSFT | 73.25 | <u>78.75</u> | 81.40 | 50.60 | 74.45 | 70.17 | 71.43 |
| | MCDPO | 87.75 | 94.25 | 93.00 | 51.75 | 83.50 | 76.75 | 81.16 |

Table 2. Main Results on SDXL (win rates vs. SDXL baseline).

| Datasets | Models | PickScore | Aesthetic | HPSv2 | CLIP | ImageReward | MPS | Average |
|--------------|------------|--------------|--------------|--------------|--------------|--------------|--------------|--------------|
| PickV2 | Diff. DPO* | <u>71.60</u> | 49.20 | 72.92 | 61.24 | 68.64 | <u>60.36</u> | <u>63.99</u> |
| | MAPO* | 50.65 | <u>56.00</u> | <u>80.00</u> | 59.15 | 74.19 | 52.26 | 62.02 |
| | DSPO | 68.80 | 44.76 | 71.80 | 60.60 | 74.24 | 44.77 | 60.82 |
| | MCSFT | 50.72 | 37.24 | 72.36 | 59.12 | 66.20 | 45.96 | 55.26 |
| | MCDPO | 74.92 | 63.40 | 85.84 | 58.16 | 77.72 | 64.31 | 70.72 |
| PartiPrompts | Diff. DPO* | 64.09 | 54.66 | 67.34 | 58.21 | 68.44 | <u>62.70</u> | 62.57 |
| | MAPO* | 50.20 | 68.07 | <u>76.47</u> | 52.38 | 69.73 | 53.10 | 61.65 |
| | DSPO | 64.58 | 56.92 | 71.26 | <u>56.67</u> | 78.49 | 53.49 | 63.56 |
| | MCSFT | 46.69 | 46.32 | 71.51 | 55.27 | 64.28 | 51.96 | 56.81 |
| | MCDPO | 72.06 | <u>66.67</u> | 82.41 | 55.56 | <u>73.47</u> | 64.01 | 69.03 |
| HPDv2 | Diff. DPO* | 67.80 | 54.85 | 72.10 | 55.20 | 67.85 | <u>57.53</u> | 62.55 |
| | MAPO* | 50.80 | 56.55 | <u>84.35</u> | 54.25 | 70.75 | 48.35 | 60.84 |
| | DSPO | 70.30 | 50.35 | 78.80 | 54.75 | <u>73.85</u> | 53.75 | 63.63 |
| | MCSFT | 51.85 | 40.10 | 78.30 | 54.75 | 66.95 | 46.98 | 56.48 |
| | MCDPO | 76.40 | 69.25 | 90.60 | <u>54.85</u> | 75.20 | 69.26 | 72.59 |

4. Experiments

4.1. Experimental Setup

Training Dataset. Following the previous works, we adopt Pick-a-Pic v2 [8], containing 1M human-preference image pairs as the training dataset. We augment each pair with four model-based reward dimensions: aesthetic quality (Aesthetic Predictor [20]), semantic alignment (CLIP [17]), overall quality (HPSv2 [26]), and prompt alignment (PickScore [8]). For our method, the 5-dimensional preference outcome vector γ is then constructed by encoding the win/lose/tie status for the original human label alongside these four proxy reward dimensions. We use 18% of the data ($\sim 180K$ pairs) for StableDiffusion1.5 (SD1.5) [19] and 3% ($\sim 30K$ pairs) for SDXL [16].

Configuration. Training proceeds in two phases: (1) MCSFT pre-training and (2) MCDPO alignment. The total computational time, including the prior MCSFT pretraining, was 8 hours for SD1.5 and 16 hours for SDXL with 2x

A100 80GB GPUs. Other implementation details are provided in the Appendix.

Evaluation. To evaluate MCDPO’s effectiveness, we compare against existing baselines trained on the Pick-a-Pic v2 dataset: Diffusion-DPO [23], Diffusion-KTO [11], MAPO [7], and DSPO [33]. Following standard convention, we test text-to-image generation on Pick-a-Pic v2 test set [8], PartiPrompts [31], and HPDv2 test set [26], measuring performance with PickScore, LAION Aesthetic Score, HPSv2, CLIP, ImageReward [27], and MPS [32].

4.2. Main Results

As shown in Table 1, our method, MCDPO, demonstrates dominant performance on the SD1.5 benchmark, significantly outperforming all baselines (Diffusion-DPO, Diffusion-KTO, and DSPO) across every test set. We observe substantial gains in both PickScore and HPSv2. The most notable improvement is in the aesthetic score, which shows a massive performance gain over existing methods.

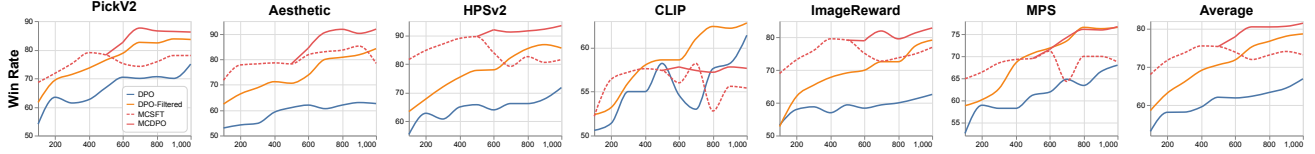


Figure 2. MCDPO learns efficiently from reward-conflicting pairs. Unlike DPO (degraded by conflicts) and DPO-Filtered (wastes samples avoiding conflicts), MCDPO resolves conflicts fundamentally and outperforms both baselines with the same data budget.

Furthermore, MCDPO achieves consistent gains on ImageReward and MPS, metrics not used as a direct reward dimension, indicating strong generalization capabilities.

This significant performance advantage is maintained on SDXL, as detailed in Table 2. MCDPO again outperforms all baselines on PickScore, HPSv2, and MPS, achieving the highest average score by a large margin

While MCDPO achieves substantial improvements across human-preference metrics, CLIP scores show modest gains that warrant explanation. Importantly, Table 5 demonstrates that MCDPO successfully learns CLIP optimization. When applying test-time guidance targeting CLIP specifically, our model achieves 59.0%, notably higher than baseline DPO (57.8%). This proves the model has learned a disentangled CLIP representation. However, when optimizing all dimensions simultaneously, CLIP score moderates to 57.6%. This reflects the fundamental nature of multi-objective optimization. Achieving peak performance across all metrics simultaneously requires balanced compromise. The slight moderation in CLIP (while remaining competitive with baselines) enables dramatic improvements in aesthetics (91.8%), HPSv2 (93.4%), ImageReward (82.9%), and MPS (76.7%). Critically, our conditional framework allows users to dynamically adjust this trade-off at inference, boosting CLIP to 59.0% when semantic alignment is prioritized, or maximizing aesthetics when preferred.

A key advantage of MCDPO is sample efficiency through effective conflict resolution. Figure 2 compares three training regimes using 18% of Pick-a-Pic v2 data: (1) Standard DPO on randomly sampled 18%, (2) DPO-Filtered on conflict-free pairs only (18% of full data), and (3) MCDPO on randomly sampled 18%. Despite identical compute budgets, MCDPO significantly outperforms both baselines, including DPO-Filtered, which explicitly avoids conflicting signals. This demonstrates that MCDPO transforms conflict pairs from obstacles into effective training signals, enabling strong performance with substantially less data than standard approaches require. Furthermore, we observe that the MCSFT pre-training (shown up to 1000 steps) alone is insufficient. Figure 2 shows that extending MCSFT training leads to performance degradation and fluctuation, confirming it primarily serves to initialize the reward conditioning module. This highlights that the MCDPO alignment objective itself is critical for achieving stable and superior performance.

Table 3. Ablation study of MCDPO components on PickV2.

| | Pick | Aes | HPS | CLIP | IR | MPS | Avg |
|------------------|------|-------------|------|-------------|------|------|------|
| MCDPO | 86.2 | 91.8 | 93.4 | 57.6 | 83.0 | 76.7 | 81.1 |
| - reward dropout | 87.2 | 96.0 | 92.2 | <u>49.2</u> | 79.2 | 77.1 | 80.1 |
| - MCSFT | 53.8 | 79.2 | 55.0 | 48.8 | 55.8 | 70.7 | 60.5 |
| - CAR module | 80.0 | 90.0 | 80.8 | 45.8 | 69.8 | 54.4 | 70.1 |

Furthermore, we visualize the qualitative performance of MCDPO against baseline methods on both SD1.5 and SDXL, as shown in Figure 3 and Figure 4, respectively. Across both model architectures, our method demonstrates a clear superiority in generating images that are more aesthetically pleasing and detailed.

4.3. Analysis

Component Ablation Study. We conduct an ablation study to validate the contribution of MCDPO’s core components: dimensional reward dropout, the context-aware reward module, and the MCSFT pre-training stage. The result is shown in Table 3

First, removing the dimensional reward dropout leads to a seemingly dominant aesthetic score (96.0%) but causes a catastrophic collapse in the CLIP score (49.2%). We believe this is a clear case of the gradient domination problem discussed in Section 3.3. The easier aesthetic dimension appears to saturate the learning signal, preventing the harder CLIP dimension from being optimized. Our reward dropout technique effectively mitigates this issue, ensuring balanced optimization and contributing significantly to the superior overall performance.

Removing MCSFT pre-training causes a drastic performance decline, showing non-initialized conditioning is disruptive. However, MCSFT alone is insufficient. On SDXL, MCSFT performs poorly (Avg 57.13), while the full MCDPO model achieves 72.01 (Table 2), proving the MCDPO alignment stage itself is critical.

Finally, ablating the Context-Aware Reward conditioning module Equation (19) causes a severe performance drop in all metrics except for aesthetics. These affected metrics (PickScore, HPS, CLIP, IR) measure alignment between the image and the text prompt. This result confirms our hypothesis: to condition on rewards like semantic alignment effectively, the model must be aware of both the image and the text context, validating the design of our module.

Multi-dimensional Learning. Table 4 validates the effectiveness of our approach, multi-dimensional learning, by

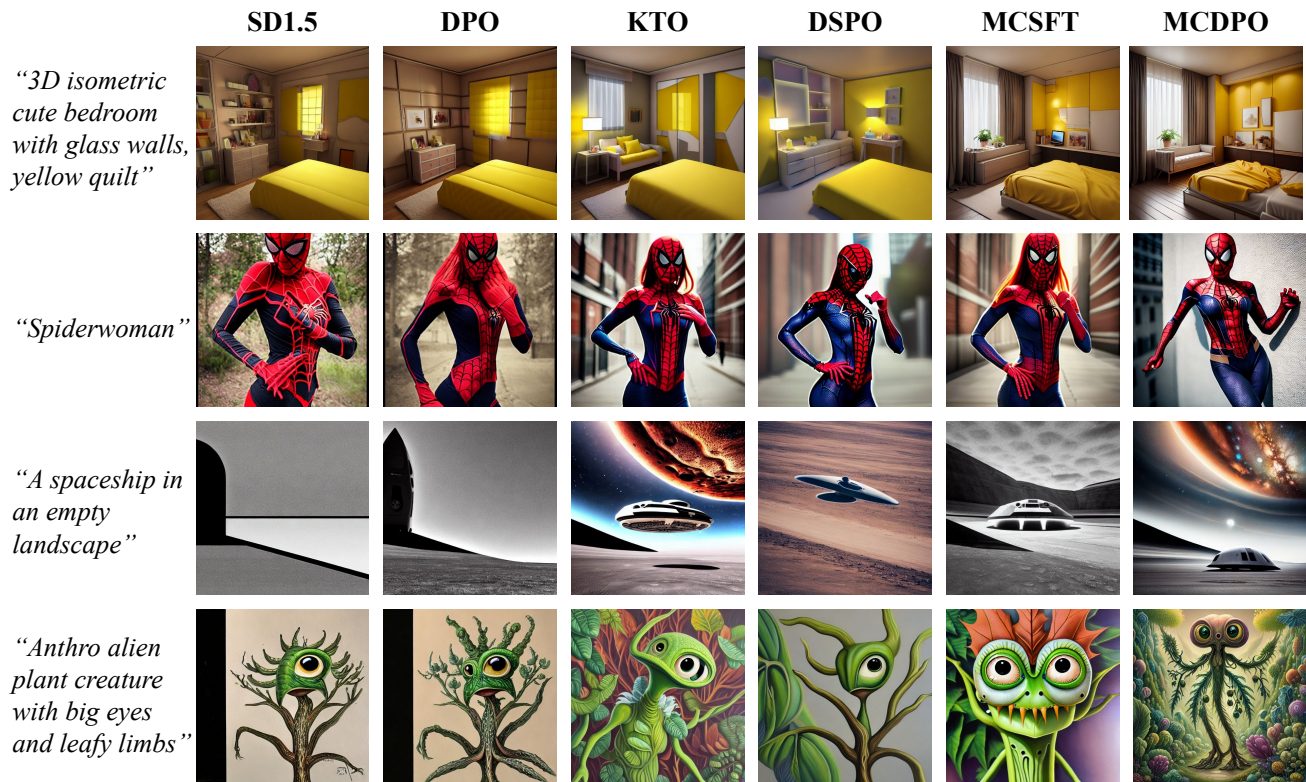


Figure 3. Qualitative results of SD1.5.

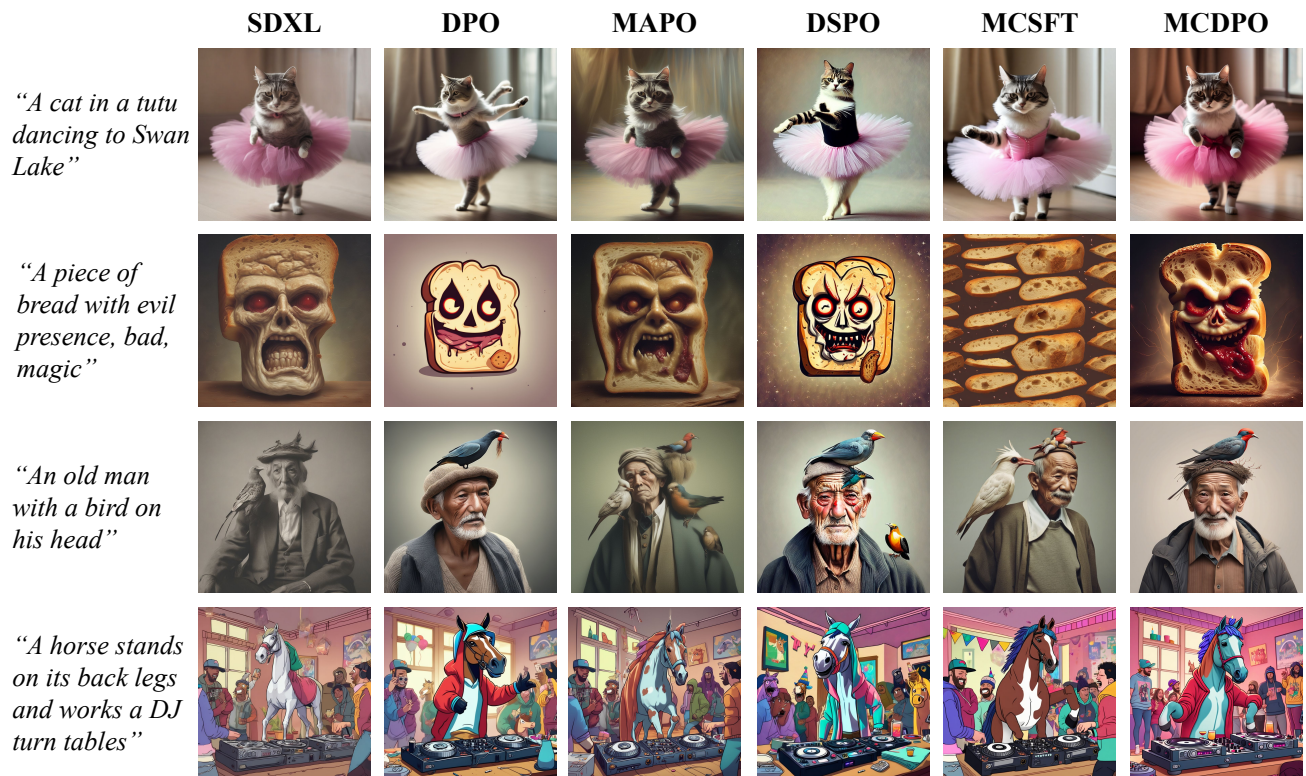


Figure 4. Qualitative results of SDXL.

Table 4. Comparison of MCDPO (ALL) against single-dimension specialist models.

| Reward | Pick | Aes | HPS | CLIP | IR | MPS | Avg |
|--------|-------------|-------------|-------------|-------------|-------------|-------------|-------------|
| Human | 79.0 | 79.8 | 86.6 | 46.8 | 75.8 | 73.2 | 73.5 |
| Pick | 80.6 | 82.8 | 88.6 | 49.0 | 76.8 | 74.7 | 75.4 |
| Aes | 79.6 | 88.0 | 87.2 | 49.2 | 76.2 | 72.4 | 75.4 |
| HPS | 77.8 | 81.8 | 88.0 | 50.2 | 77.6 | 73.3 | 74.7 |
| CLIP | 75.4 | 79.4 | 84.4 | 49.2 | 76.0 | 70.9 | 72.5 |
| ALL | 86.2 | 91.8 | 93.4 | 57.6 | 82.9 | 76.7 | 81.1 |

comparing MCDPO trained on all reward dimensions simultaneously (ALL) against specialist models trained on only a single reward dimension. Remarkably, the MCDPO (ALL) model not only achieves the highest average score but also outperforms every individual specialist model even on its own specialized metric. For example, the MCDPO (ALL) model (Aesthetic win-rate 91.8) surpasses the model trained exclusively on ‘Aesthetic’ rewards (Aesthetic win-rate 88.0). This finding strongly substantiates our core hypothesis. It suggests that training DPO on even a single dimension still fails to achieve optimal performance due to implicit reward conflicts with other unstated dimensions. The model struggles because it cannot resolve these conflicts that it is not conditioned to understand. In contrast, MCDPO resolves this issue by explicitly conditioning on and disentangling all potential conflict axes. This allows the model to properly optimize each dimension individually, which leads to state-of-the-art performance across all metrics.

Multi-dimensional Inference. As demonstrated in Table 5, our single model, trained to disentangle reward axes, can perform dynamic preference-enhancing sampling at test-time as described in Section 3.4. When steering the sampling to amplify only a specific dimension, we observe distinct and controlled behaviors. Critically, when enhancing CLIP, the model achieves 59.0% higher than both the baseline DPO (57.8%) and the all-dimension optimization (57.6%). This demonstrates that MCDPO has successfully learned a disentangled representation of CLIP rewards and can boost this dimension when desired. Similarly, enhancing Aes (Aesthetic) generates samples with exceptionally high aesthetic scores (95.8%), validating dimension-specific control. Notably, when enhancing PickScore and HPSv2, their corresponding scores increase as expected. However, we also observe a concurrent rise in CLIP, ImageReward, and MPS scores. We attribute this to the nature of PickScore and HPSv2 as holistic metrics that evaluate overall image quality, which naturally correlates with other reward axes. This result validates that our model has successfully learned to disentangle each dimension, allowing it to leverage this capability at test-time to perform guided sampling that enhances the reward for a targeted dimension.

Implicit Reward Modeling Table 6 demonstrates that MCDPO accurately models implicit reward functions for each dimension. MCDPO achieves comparable accuracy to

Table 5. Test-time reward optimization by guiding the MCDPO (ALL) model towards specific target dimensions.

| Reward | Pick | Aes | HPS | CLIP | IR | MPS | Avg |
|--------|-------------|-------------|-------------|-------------|-------------|-------------|-------------|
| Human | 78.6 | 79.0 | 83.2 | 55.2 | 73.8 | 67.7 | 72.9 |
| Pick | 78.2 | 79.0 | 85.0 | 57.6 | 78.4 | 69.9 | 74.7 |
| Aes | 77.4 | 95.8 | 79.0 | 49.2 | 73.0 | 68.9 | 73.8 |
| HPS | 77.0 | 79.4 | 85.6 | 59.0 | 77.8 | 71.1 | 74.9 |
| CLIP | 76.4 | 76.6 | 85.0 | 59.0 | 75.0 | 67.8 | 73.3 |
| ALL | 86.2 | 91.8 | 93.4 | 57.6 | 82.9 | 76.7 | 81.1 |

Table 6. Implicit reward accuracy comparison between MCDPO and specialist models across different reward dimensions.

| | Human | Pick | Aes | HPS | CLIP |
|-------------|-------|------|------|------|------|
| Specialists | 57.8 | 61.0 | 67.1 | 58.2 | 59.9 |
| MCDPO | 58.7 | 61.7 | 66.2 | 55.0 | 59.4 |
| MCDPO win | 58.5 | 58.7 | 50.8 | 52.9 | 59.4 |
| MCDPO lose | 42.2 | 41.0 | 53.3 | 46.8 | 56.8 |

specialist models trained on individual dimensions, while being significantly more computationally efficient by learning all dimensions within a single network. Furthermore, our conditional DPO framework simultaneously models both r^w (preferred) and r^l (non-preferred) implicit reward models as described in Equation (15). Leveraging both models together yields performance gains over using either model alone. For example, in the Aesthetic dimension, while the win-only model achieves 50.8% and the lose-only model achieves 53.3%, combining both models substantially improves accuracy to 66.2%. Similarly, for Human and PickScore dimensions, despite the lose models showing relatively lower accuracies (42.2% and 41.0% respectively), combining them with the win models consistently yields performance improvements.

5. Discussion

Conclusion. We introduced Multi Reward Conditional DPO (MCDPO), a framework that fundamentally resolves the reward conflict inherent in the standard Bradley-Terry formulation. By explicitly conditioning on preference outcome vectors, our approach transforms conflicting data pairs into robust training signals for disentangled alignment. Empirical results confirm that MCDPO achieves state-of-the-art performance and superior sample efficiency. Ultimately, this conditional framework offers a scalable and unified solution for precise and multi-dimensional control in generative model alignment.

Limitations. While MCDPO effectively disentangles reward axes, the method relies on the availability of reliable proxy reward models to construct the preference outcome vector during training. The quality of the final alignment is therefore upper-bounded by the accuracy of these proxy judges. Additionally, unlike standard DPO, which utilizes binary human labels directly, our approach introduces a pre-processing overhead to generate multi-dimensional reward scores for the training data.

References

- [1] Kevin Black, Michael Janner, Yilun Du, Ilya Kostrikov, and Sergey Levine. Training diffusion models with reinforcement learning. *arXiv preprint arXiv:2305.13301*, 2023. 1
- [2] Ralph Allan Bradley and Milton E Terry. Rank analysis of incomplete block designs: I. the method of paired comparisons. *Biometrika*, 39(3/4):324–345, 1952. 2
- [3] Sayak Ray Chowdhury, Anush Kini, and Nagarajan Nataraajan. Provably robust dpo: Aligning language models with noisy feedback. *arXiv preprint arXiv:2403.00409*, 2024. 3
- [4] Haoran Gu, Handing Wang, Yi Mei, Mengjie Zhang, and Yaochu Jin. Paretohd: Fast offline multiobjective alignment of large language models using pareto high-quality data. *arXiv preprint arXiv:2504.16628*, 2025. 1, 3
- [5] Jonathan Ho and Tim Salimans. Classifier-free diffusion guidance. *arXiv preprint arXiv:2207.12598*, 2022. 2
- [6] Jonathan Ho, Ajay Jain, and Pieter Abbeel. Denoising diffusion probabilistic models. *Advances in neural information processing systems*, 33:6840–6851, 2020. 2
- [7] Jiwoong Hong, Sayak Paul, Noah Lee, Kashif Rasul, James Thorne, and Jongheon Jeong. Margin-aware preference optimization for aligning diffusion models without reference, 2024. 5
- [8] Yuval Kirstain, Adam Polyak, Uriel Singer, Shahbuland Matiana, Joe Penna, and Omer Levy. Pick-a-pic: An open dataset of user preferences for text-to-image generation. *Advances in Neural Information Processing Systems*, 36:36652–36663, 2023. 5, 1
- [9] Kimin Lee, Hao Liu, Moonkyung Ryu, Olivia Watkins, Yuqing Du, Craig Boutilier, Pieter Abbeel, Mohammad Ghavamzadeh, and Shixiang Shane Gu. Aligning text-to-image models using human feedback. *arXiv preprint arXiv:2302.12192*, 2023. 1
- [10] Kyungmin Lee, Xiahong Li, Qifei Wang, Junfeng He, Junjie Ke, Ming-Hsuan Yang, Irfan Essa, Jinwoo Shin, Feng Yang, and Yinxiao Li. Calibrated multi-preference optimization for aligning diffusion models. In *Proceedings of the Computer Vision and Pattern Recognition Conference*, pages 18465–18475, 2025. 1, 3
- [11] Shufan Li, Konstantinos Kallidromitis, Akash Gokul, Yusuke Kato, and Kazuki Kozuka. Aligning diffusion models by optimizing human utility. In *The Thirty-eighth Annual Conference on Neural Information Processing Systems*, 2024. 5
- [12] Aixin Liu, Bei Feng, Bing Xue, Bingxuan Wang, Bochao Wu, Chengda Lu, Chenggang Zhao, Chengqi Deng, Chenyu Zhang, Chong Ruan, et al. Deepseek-v3 technical report. *arXiv preprint arXiv:2412.19437*, 2024. 1
- [13] Xingzhou Lou, Junge Zhang, Jian Xie, Lifeng Liu, Dong Yan, and Kaiqi Huang. Spo: Multi-dimensional preference sequential alignment with implicit reward modeling. *arXiv preprint arXiv:2405.12739*, 2024. 1, 3
- [14] OpenAI, :, Sandhini Agarwal, Lama Ahmad, Jason Ai, Sam Altman, Andy Applebaum, Edwin Arbus, Rahul K. Arora, Yu Bai, Bowen Baker, Haiming Bao, Boaz Barak, Ally Bennett, Tyler Bertao, Nivedita Brett, Eugene Brevdo, Greg Brockman, Sebastien Bubeck, Che Chang, Kai Chen, Mark Chen, Enoch Cheung, Aidan Clark, Dan Cook, Marat Dukhan, Casey Dvorak, Kevin Fives, Vlad Fomenko, Timur Garipov, Kristian Georgiev, Mia Glaese, Tarun Gogineni, Adam Goucher, Lukas Gross, Katia Gil Guzman, John Hallman, Jackie Hehir, Johannes Heidecke, Alec Helyar, Haitang Hu, Romain Huet, Jacob Huh, Saachi Jain, Zach Johnson, Chris Koch, Irina Kofman, Dominik Kundel, Jason Kwon, Volodymyr Korylov, Elaine Ya Le, Guillaume Leclerc, James Park Lennon, Scott Lessans, Mario Lezcano-Casado, Yuanzhi Li, Zhuohan Li, Ji Lin, Jordan Liss, Lily, Liu, Jiancheng Liu, Kevin Lu, Chris Lu, Zoran Martinovic, Lindsay McCallum, Josh McGrath, Scott McKinney, Aidan McLaughlin, Song Mei, Steve Mostovoy, Tong Mu, Gideon Myles, Alexander Neitz, Alex Nichol, Jakub Pachocki, Alex Paino, Dana Palmie, Ashley Pantuliano, Giambattista Parascandolo, Jongsoo Park, Leher Pathak, Carolina Paz, Ludovic Peran, Dmitry Pimenov, Michelle Pokrass, Elizabeth Proehl, Huida Qiu, Gaby Raila, Filippo Raso, Hongyu Ren, Kimmy Richardson, David Robinson, Bob Rotsted, Hadi Salman, Suvansh Sanjeev, Max Schwarzer, D. Sculley, Harshit Sikchi, Kendal Simon, Karan Singhal, Yang Song, Dane Stuckey, Zhiqing Sun, Philippe Tillet, Sam Toizer, Foivos Tsimpourlas, Nikhil Vyas, Eric Wallace, Xin Wang, Miles Wang, Olivia Watkins, Kevin Weil, Amy Wendling, Kevin Whinnery, Cedric Whitney, Hannah Wong, Lin Yang, Yu Yang, Michihiro Yasunaga, Kristen Ying, Wojciech Zaremba, Wenting Zhan, Cyril Zhang, Brian Zhang, Eddie Zhang, and Shengjia Zhao. gpt-oss-120b & gpt-oss-20b model card, 2025. 1
- [15] Long Ouyang, Jeffrey Wu, Xu Jiang, Diogo Almeida, Carroll Wainwright, Pamela Mishkin, Chong Zhang, Sandhini Agarwal, Katarina Slama, Alex Ray, et al. Training language models to follow instructions with human feedback. *Advances in neural information processing systems*, 35:27730–27744, 2022. 1
- [16] Dustin Podell, Zion English, Kyle Lacey, Andreas Blattmann, Tim Dockhorn, Jonas Müller, Joe Penna, and Robin Rombach. Sdxl: Improving latent diffusion models for high-resolution image synthesis. *arXiv preprint arXiv:2307.01952*, 2023. 5
- [17] Alec Radford, Jong Wook Kim, Chris Hallacy, Aditya Ramesh, Gabriel Goh, Sandhini Agarwal, Girish Sastry, Amanda Askell, Pamela Mishkin, Jack Clark, et al. Learning transferable visual models from natural language supervision. In *International conference on machine learning*, pages 8748–8763. Pmlr, 2021. 5
- [18] Rafael Rafailov, Archit Sharma, Eric Mitchell, Christopher D Manning, Stefano Ermon, and Chelsea Finn. Direct preference optimization: Your language model is secretly a reward model. *Advances in neural information processing systems*, 36:53728–53741, 2023. 1, 2
- [19] Robin Rombach, Andreas Blattmann, Dominik Lorenz, Patrick Esser, and Björn Ommer. High-resolution image synthesis with latent diffusion models. In *Proceedings of the IEEE/CVF Conference on Computer Vision and Pattern Recognition (CVPR)*, pages 10684–10695, 2022. 5
- [20] Christoph Schuhmann. Laion-aesthetics. <https://>

- laion.ai/blog/laion-aesthetics/, 2022. Accessed: 2023 - 11- 10. [5](#)
- [21] Yang Song, Jascha Sohl-Dickstein, Diederik P Kingma, Abhishek Kumar, Stefano Ermon, and Ben Poole. Score-based generative modeling through stochastic differential equations. *arXiv preprint arXiv:2011.13456*, 2020. [2](#)
- [22] Jie Sun, Junkang Wu, Jiancan Wu, Zhibo Zhu, Xingyu Lu, Jun Zhou, Lintao Ma, and Xiang Wang. Robust preference optimization via dynamic target margins. *arXiv preprint arXiv:2506.03690*, 2025. [3](#)
- [23] Bram Wallace, Meihua Dang, Rafael Rafailov, Linqi Zhou, Aaron Lou, Senthil Purushwalkam, Stefano Ermon, Caiming Xiong, Shafiq Joty, and Nikhil Naik. Diffusion model alignment using direct preference optimization. In *Proceedings of the IEEE/CVF Conference on Computer Vision and Pattern Recognition*, pages 8228–8238, 2024. [1](#), [2](#), [5](#)
- [24] Kaiwen Wang, Rahul Kidambi, Ryan Sullivan, Alekh Agarwal, Christoph Dann, Andrea Michi, Marco Gelmi, Yunxuan Li, Raghav Gupta, Kumar Avinava Dubey, et al. Conditional language policy: A general framework for steerable multi-objective finetuning. In *Findings of the Association for Computational Linguistics: EMNLP 2024*, pages 2153–2186, 2024. [1](#), [3](#)
- [25] Junkang Wu, Yuexiang Xie, Zhengyi Yang, Jiancan Wu, Jinyang Gao, Bolin Ding, Xiang Wang, and Xiangnan He. β -dpo: Direct preference optimization with dynamic β . *Advances in Neural Information Processing Systems*, 37: 129944–129966, 2024. [3](#)
- [26] Xiaoshi Wu, Yiming Hao, Keqiang Sun, Yixiong Chen, Feng Zhu, Rui Zhao, and Hongsheng Li. Human preference score v2: A solid benchmark for evaluating human preferences of text-to-image synthesis. *CoRR*, 2023. [5](#)
- [27] Jiazheng Xu, Xiao Liu, Yuchen Wu, Yuxuan Tong, Qinkai Li, Ming Ding, Jie Tang, and Yuxiao Dong. Imagereward: Learning and evaluating human preferences for text-to-image generation. *Advances in Neural Information Processing Systems*, 36:15903–15935, 2023. [1](#), [5](#)
- [28] An Yang, Anfeng Li, Baosong Yang, Beichen Zhang, Binyuan Hui, Bo Zheng, Bowen Yu, Chang Gao, Chengen Huang, Chenxu Lv, Chujie Zheng, Dayiheng Liu, Fan Zhou, Fei Huang, Feng Hu, Hao Ge, Haoran Wei, Huan Lin, Jialong Tang, Jian Yang, Jianhong Tu, Jianwei Zhang, Jianxin Yang, Jiayi Yang, Jing Zhou, Jingren Zhou, Junyang Lin, Kai Dang, Keqin Bao, Kexin Yang, Le Yu, Lianghao Deng, Mei Li, Mingfeng Xue, Mingze Li, Pei Zhang, Peng Wang, Qin Zhu, Rui Men, Ruize Gao, Shixuan Liu, Shuang Luo, Tianhao Li, Tianyi Tang, Wenbiao Yin, Xingzhang Ren, Xinyu Wang, Xinyu Zhang, Xuancheng Ren, Yang Fan, Yang Su, Yichang Zhang, Yinger Zhang, Yu Wan, Yuqiong Liu, Zekun Wang, Zeyu Cui, Zhenru Zhang, Zhipeng Zhou, and Zihan Qiu. Qwen3 technical report, 2025. [1](#)
- [29] Rui Yang, Xiaoman Pan, Feng Luo, Shuang Qiu, Han Zhong, Dong Yu, and Jianshu Chen. Rewards-in-context: Multi-objective alignment of foundation models with dynamic preference adjustment. *arXiv preprint arXiv:2402.10207*, 2024. [1](#), [3](#)
- [30] Hu Ye, Jun Zhang, Sibao Liu, Xiao Han, and Wei Yang. Ip-adapter: Text compatible image prompt adapter for text-to-image diffusion models. *arXiv preprint arXiv:2308.06721*, 2023. [4](#)
- [31] Jiahui Yu, Yuanzhong Xu, Jing Yu Koh, Thang Luong, Gunjan Baid, Zirui Wang, Vijay Vasudevan, Alexander Ku, Yinfei Yang, Burcu Karagol Ayan, et al. Scaling autoregressive models for content-rich text-to-image generation. *Trans. Mach. Learn. Res.*, 2022. [5](#)
- [32] Sixian Zhang, Bohan Wang, Junqiang Wu, Yan Li, Tingting Gao, Di Zhang, and Zhongyuan Wang. Learning multi-dimensional human preference for text-to-image generation. In *Proceedings of the IEEE/CVF Conference on Computer Vision and Pattern Recognition*, pages 8018–8027, 2024. [5](#)
- [33] Huaisheng Zhu, Teng Xiao, and Vasant G Honavar. DSPO: Direct score preference optimization for diffusion model alignment. In *The Thirteenth International Conference on Learning Representations*, 2025. [5](#)

Multi-dimensional Preference Alignment by Conditioning Reward Itself

Supplementary Material

A. Analysis of Reward Correlation and Conflict

To provide a quantitative foundation for our paper’s core premise, we analyzed the relationships between the reward dimensions used in our training data. The central motivation for MCDPO is the existence of "reward conflict," where different preference axes provide contradictory optimization signals. We computed the Pearson correlation matrix for the five primary reward dimensions across our training set (derived from Pick-a-Pic v2 [8]) in Table 7.

Table 7. Pearson correlation matrix of the five reward dimensions used in the training dataset.

| | Human | PickScore | Aesthetic | HPSv2 | CLIP |
|-----------|--------|-----------|-----------|--------|---------|
| Human | 1.0000 | 0.2649 | 0.0097 | 0.0960 | 0.1277 |
| PickScore | 0.2649 | 1.0000 | -0.0501 | 0.4683 | 0.4174 |
| Aesthetic | 0.0097 | -0.0501 | 1.0000 | 0.1083 | -0.0662 |
| HPSv2 | 0.0960 | 0.4683 | 0.1083 | 1.0000 | 0.4325 |
| CLIP | 0.1277 | 0.4174 | -0.0662 | 0.4325 | 1.0000 |

This correlation matrix provides direct, quantitative validation for our paper’s thesis. The most critical finding is the Aesthetic dimension, which shows a near-zero or slightly negative correlation with all other preference metrics, including PickScore (-0.0501), CLIP Score (-0.0662), and Human Preference (0.0097). This data proves that optimizing for what a human prefers provides no signal for optimizing aesthetics. This is the "reward conflict" we identify. A standard DPO model, which aggregates these signals into a single scalar, is forced to average these contradictory gradients, leading to suboptimal performance on some axes. While PickScore, CLIP Score, and HPS Score show moderate positive correlations (0.41-0.46), they are far from 1.0, indicating they capture related but distinct aspects of quality and semantic alignment.

Furthermore, the Human Preference label, which serves as the ground truth alignment target, shows only a weak correlation with any single proxy model (e.g., 0.1277 with CLIP Score and 0.0960 with HPS Score). This finding suggests the complexity of the alignment task, as it indicates that no single proxy serves as a strong substitute for the true, complex human preference. This suggests the model must learn from a combination of noisy, low-correlation, and conflicting signals. These findings collectively suggest that reward conflict is a measurable property of the data, not just a theoretical edge case. This motivates a solution beyond simple aggregation and provides a strong justification for our proposed method, MCDPO, which is explicitly designed to disentangle and optimize these axes independently.

B. Single Dimensional Training without Conditioning

Table 8. Comparison of single-dimension DPO specialists trained without conditioning. We report win rates for each specialist, their parameter-averaged model (Merged), and our MCDPO for reference.

| | PickScore | Aesthetic | HPSv2 | CLIP | ImageReward | MPS | Average |
|-----------|-------------|-------------|-------------|-------------|-------------|-------------|-------------|
| Human | <u>75.0</u> | 62.6 | 71.8 | 60.4 | <u>62.6</u> | <u>68.0</u> | <u>66.7</u> |
| PickScore | 72.6 | 63.4 | <u>72.0</u> | <u>59.2</u> | 57.6 | 66.6 | 65.2 |
| Aesthetic | 69.8 | <u>66.2</u> | 66.4 | 56.4 | 59.6 | 66.0 | 64.1 |
| HPSv2 | 69.8 | 63.8 | 70.0 | 54.6 | 59.6 | 65.9 | 64.0 |
| CLIP | 69.2 | 62.4 | 67.6 | 58.6 | 58.8 | 63.2 | 63.3 |
| Merged | 73.4 | 63.6 | 70.0 | 56.0 | 62.0 | 67.8 | 63.8 |
| MCDPO | 86.2 | 91.8 | 93.4 | 57.6 | 82.9 | 76.7 | 81.1 |

To establish a robust naive baseline, we trained five independent specialist models using the standard DPO formulation. Each model was trained to optimize for only one reward dimension, specifically Human, PickScore, Aesthetic, HPSv2, or CLIP. These models do not utilize our proposed conditional module. We also evaluated a Merged model, which is created by uniformly averaging the parameters of all five specialist models.

The results are presented in Table 8. The Merged model, which represents a strong ensemble baseline, achieves an average win rate of 63.8, which is substantially outperformed by our full MCDPO model’s average of 81.1. This suggests that our preference vector-based conditional training framework is a more effective and efficient method for multi-dimensional alignment than the naive parameter averaging ensemble technique.

This performance gap is further explained by comparing MCDPO to the individual specialists. MCDPO outperforms the specialists on nearly all dimensions, often by a large margin. For example, the Aesthetic specialist achieves only 66.2 on its own metric, whereas MCDPO achieves 91.8. This trend holds for PickScore, HPSv2, ImageReward, and MPS. We note that MCDPO’s CLIP score is slightly lower than that of some specialists, which aligns with the findings in our main paper. This strongly supports our central hypothesis that standard DPO struggles with implicit reward conflicts, which MCDPO successfully resolves to achieve a superior overall balance.

C. Implementation Details

Our training process consists of two main phases: Multi-reward Conditional Supervised Fine-Tuning (MCSFT) and Multi-reward Conditional Direct Preference Optimization (MCDPO). In the initial MCSFT stage, the parameters of the original U-Net are frozen, and only the conditioning module described in Section 3.5 of the main paper is trained. For SD1.5, we train for 500 steps with a batch size of 384, 100 warmup steps, and a 1e-8 learning rate, which is linearly scaled with the batch size. For SDXL, we train for 200 steps with a batch size of 64. During this stage, we apply a reward condition dropout rate of 0.1 except Human Preference and a text condition dropout rate of 0.2. Following this, in the MCDPO stage, all model parameters, including the U-Net and the conditioning module, are fine-tuned. The conditioning module is initialized from the weights obtained during the MCSFT pre-training. We train this stage for 500 steps with a DPO β of 6000 and 100 warmup steps. We apply dimensional reward dropout with specific rates: 0.15 for CLIP, 0.2 for the other model-based rewards, and 0.0 (no dropout) for the human preference dimension. For SD1.5, we use a batch size of 384 and a 1e-9 learning rate. For SDXL, we use a batch size of 64 and a 5e-9 learning rate, with linear scaling applied to the learning rate based on batch size in this stage as well. The total combined training time for both stages, using two A100 80GB GPUs, was 8 hours for the SD1.5 model and 16 hours for the SDXL model.

D. Additional Qualitative Results

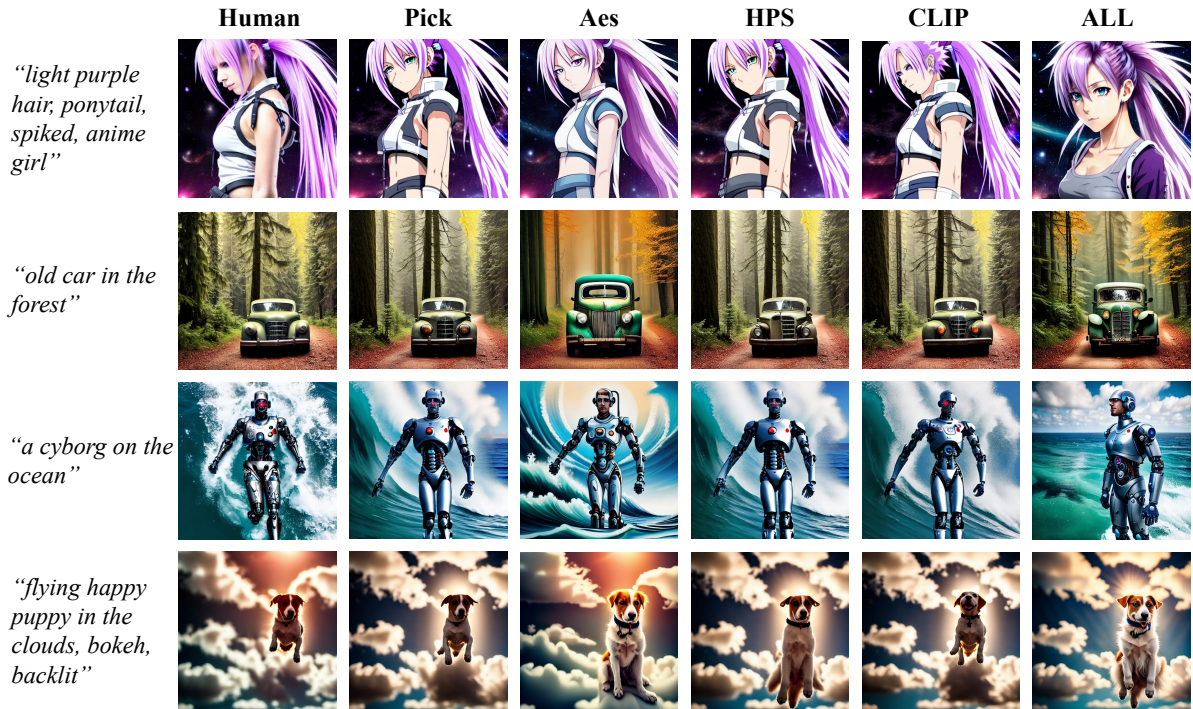


Figure 5. Visualization of single-dimensional inference (Table 4).

| | SD1.5 | DPO | KTO | DSPO | MCSFT | MCDPO |
|--|-------|-----|-----|------|-------|-------|
| <i>“Angry blue dog with bottle”</i> | | | | | | |
| <i>“a long range portrait of a cyber samurai robot”</i> | | | | | | |
| <i>“an evil entity that is made out of cheese casting a terrible spell over slices of bread”</i> | | | | | | |
| <i>“A portrait of an anime mecha robot”</i> | | | | | | |
| <i>“A hand-drawn cute gnome holding a pumpkin in an autumn disguise”</i> | | | | | | |
| <i>“3D render of a volcanic icon on a rocky background”</i> | | | | | | |
| <i>“corn elemental, created as concept art for a high fantasy setting”</i> | | | | | | |
| <i>“Small carved figurines of fantasy buildings, miniatures and standalone objects on a table”</i> | | | | | | |

Figure 6. Additional qualitative results of SD15.

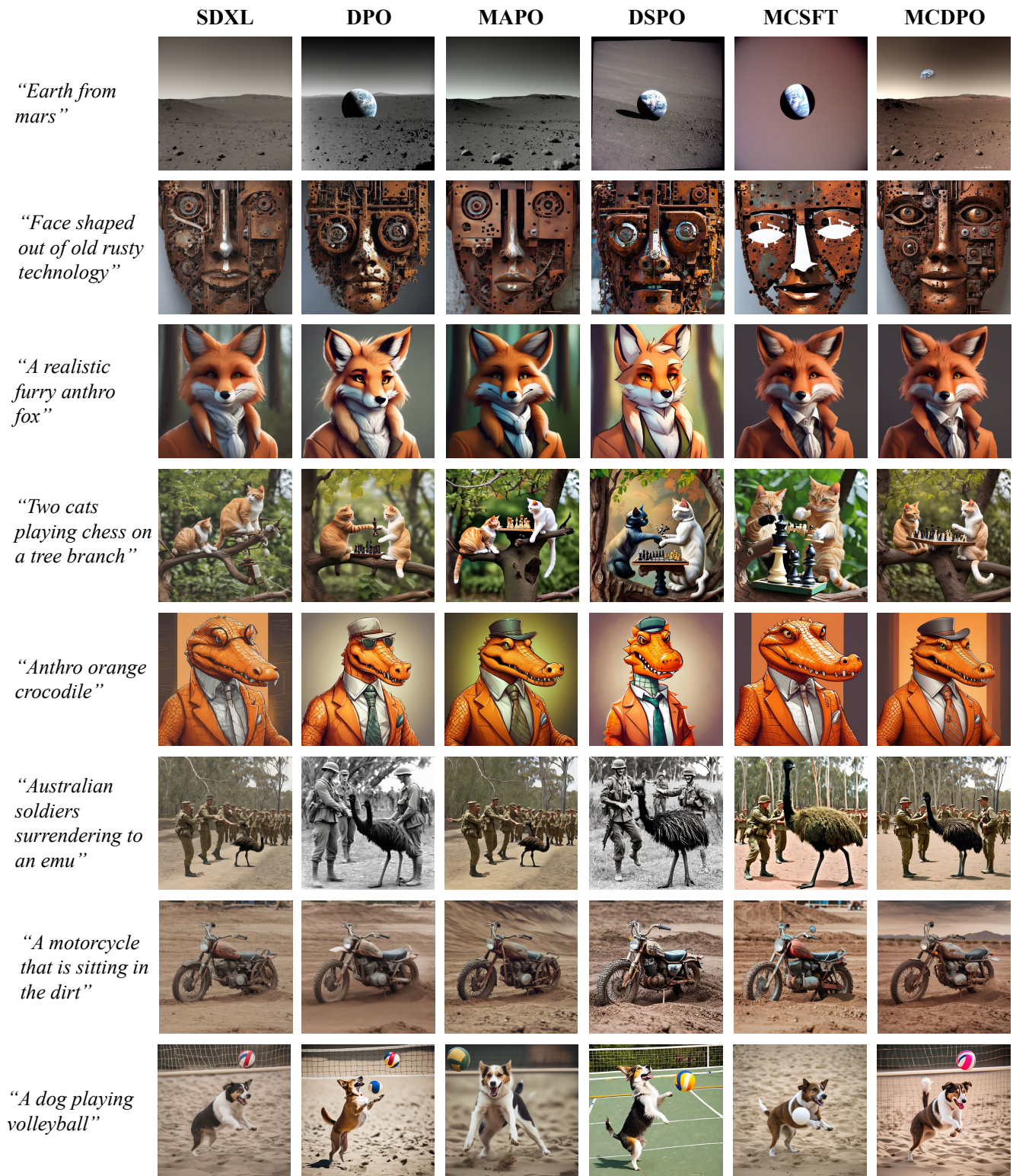


Figure 7. Additional qualitative results of SDXL.